

Numerical study of an elliptical fin inserted in a square cavity with the upper sliding surface submitted to mixed convection

Estudo numérico de uma aleta elíptica inserida em uma cavidade quadrada com a superfície superior deslizando submetida à convecção mista

Alysson Sehn^a, Cássio Spohr Fernandes^a, Elizaldo Domingues dos Santos^b, Liércio André Isoldi^b, Felipe Roman Centeno^a, Paulo Soliman^a

alysson.sehn@gmail.com, cassiospohrfernandes@gmail.com, elizaldosantos@furg.br, liercioisoldi@furg.br, frcenteno@ufrgs.br, paulo.soliman@ufrgs.com

^aUniversidade Federal do Rio Grande do Sul – UFRGS, Rua Sarmento Leite, n. 425 Porto Alegre, RS,

^bUniversidade Federal do Rio Grande – FURG, Av. Itália km 8, Rio Grande, RS, Brasil

Abstract

This paper aims to evaluate the heat transfer in a square cavity with an elliptical fin located in different positions on the cavity bottom and with different aspect ratios. The optimal geometry was analysed using the Constructal Design principle. A two-dimensional, laminar, steady state and incompressible flow was considered. The thermophysical properties were defined for $Pr = 0.71$ and they are considered constant, except for the specific mass that was determined by the Boussinesq approximation. A Rayleigh number (Ra_H) of 10^4 was adopted to define the natural convection, while a Reynolds number (Re_H) of 10^2 was adopted to define the forced convection. The fin position and its dimensions were varied, keeping the ratio of the fin area to cavity area constant ($\phi = 0.05$). The optimal geometry that maximizes the heat transfer rate was obtained through the Constructal Law. A mesh was created to solve the problem and it was adequately refined to ensure the accuracy of the results. The governing equations of the problem were solved numerically using the software ANSYS/Fluent®. This study shows that the position of the fin which maximizes the average Nusselt number in these conditions is at the point $X_1 \approx 0.3$ of the lower surface. For the aspect ratio (r) of the fin, it was observed that the minimization of the average Nusselt number occurs for r between 15 and 25. Considering all studied geometries, the optimized one can reach a performance around

Resumo

Este trabalho pretende avaliar a transferência de calor em uma cavidade quadrada com uma aleta elíptica localizada em diferentes posições no fundo da cavidade e com diferentes razões de aspecto. A geometria ideal foi analisada usando o princípio do Design Constructal. Foi considerado um escoamento bidimensional, laminar, estacionário e incompressível. As propriedades termo físicas foram definidas para $Pr = 0.71$ e são consideradas constantes, exceto para a massa específica que foi determinada pela aproximação de Boussinesq. Um número Rayleigh (Ra_H) de 10^4 foi adotado para definir a convecção natural, enquanto um número de Reynolds (Re_H) de 10^2 foi adotado para definir a convecção forçada. A posição da aleta e suas dimensões foram variadas, mantendo constante a relação entre a área da aleta e a área da cavidade ($\phi = 0,05$). A geometria ideal que maximiza a taxa de transferência de calor foi obtida através da Lei Constructal. Uma malha foi criada para resolver o problema e foi adequadamente refinada para garantir a precisão dos resultados. As equações governantes do problema foram resolvidas numericamente usando o software ANSYS / Fluent®. Este estudo mostra que a posição da aleta que maximiza o número de Nusselt médio, nessas condições, está no ponto $X_1 \approx 0,3$ da superfície inferior. Para a razão de aspecto (r) da aleta, observou-se que a minimização do número médio de Nusselt médio ocorre para r entre 15 e 25. Considerando todas as geometrias estudadas, a otimizada pode atingir um desempenho em torno de

50% superior if compared with the worst one, proving the importance of geometric evaluation in this kind of engineering problem, as well as the effectiveness of the Constructal approach.

50% superior se comparado com o pior caso, comprovando a importância da avaliação geométrica neste tipo de problema de engenharia, bem como a eficácia da abordagem Construtal.

Keywords: Heat transfer, Constructal Law, Nusselt number, elliptical fin, mixed convection

Palavras-chave: Transferência de calor, Lei Construtal, número de Nusselt, aleta elíptica, convecção mista

Introduction

The increasing evolution of technology in the industry requires more efficient components. A good example of this is the miniaturization of electronic components, requiring that large amounts of energy, in the form of heat, must be dissipated through increasingly restricted dimensions, working close to their optimum point. This inevitably results in the development of heat exchangers with high efficiency and in the knowledge of their optimal working conditions. Analyzing these aspects makes clear the relevance of the study of the application of optimization methods, such as the Constructal Law, in heat exchangers.

Heat transfer by convection, or simply convection, is the phenomenon of heat transport by the flow of a fluid, as seen in Bejan (2004). Convection can be classified as natural or forced convection, depending on how the movement of the fluid is initiated. In forced convection, the fluid is forced to flow on a surface or inside pipes by external means like pump or fan, in the natural convection any movement of the fluid is caused by natural means like the thrust effect, that is manifested with hot fluids rising and cold fluids descending (Bejan and Kraus, 2003), (Çengel and Ghajar, 2011). In addition, there is still the possibility that both processes occur concomitantly.

In the case of increased efficiency in the cooling of electronic components the fins and cavities are widely used. Fins surfaces are extended out of the body while cavities are extended surfaces inside it, and both may represent idealizations of real engineering geometries (Neto et al., 2010).

Bejan and Lorente, (2004), developed an analytical and graphical formulation with objective of maximization of flow in systems with heat and fluid flow irreversibilities and freedom to change configuration. The flow system that was adopted as global performance and with constants properties. As the configuration can change it is necessary analyze the optimal configuration. The results shown that for the geometry of the problem has an equilibrium configuration allying the flow configuration with the freedom of the architecture.

In the search for the increase of efficiency of the fins or cavities, more and more the Constructal Theory appears seeking to optimize the geometries used. The Constructal Design methodology guides the designer in the direction where the geometry performs best for the specified conditions. For example, the optimized geometry for condition set 1 is the constructal configuration of 1. For another set of conditions, the geometry developed for conditions 1 will not necessarily meet the requirements of set 2, so each set has its own constructal geometry, or optimum geometry. The Constructal Law is universal, however, the design obtained for a certain set of conditions does not (Bejan, 2000; Bejan and Lorente, 2006; Bejan and Lorente, 2008; Bejan and Zane, 2013).

The geometric optimization of T-Y-shaped cavity according constructal law. This cavity penetrates into a solid conducting wall. With a uniform generation on the solid wall the objective is to minimize the global thermal resistance between the solid and the cavity. The results shown that the optimal T-Y-shaped cavity performs approximately 108% better when compared with an optimal C-shaped cavity (Lorenzini and Rocha, 2009). Two additional lateral intrusions cooled by convection were used on the T-Y-shaped cavities. Using the constructal law the objective is to minimize the global thermal resistance between the solid and the complex assembly of cavities by give the assembly more freedom to morph, which can lead to an augmentation of the thermal performance. The results show that some configurations were practically insensitive with respect to the degrees of freedom but to the optimal geometry an improvement of approximately 45% was found (Lorenzini et al., 2012).

Lorenzini et al., (2016), investigated the effect of a rectangular fin inserted in the lower surface of a cavity submitted to mixed convection using a Constructal Design in order to find the best rectangular fin geometry. Such better geometry maximizes the Nusselt number based on the depth of the cavity. For this it was evaluated the geometry for various Rayleigh numbers ($RaH = 10^3, 10^4, 10^5$ and 10^6) when using a constant value for the Prandtl number ($Pr = 0.71$). The results showed that the mixed convection has great influence on the increase of heat transfer.

This work aims to numerically analyze the heat transfer between an elliptical fin. This fin is inserted in a square cavity with movable upper plate and all domain is submitted to a mixed convection flow. For this, the position of the fin has been varied, as well as its geometry, to obtain the ideal geometry and the location that minimizes the average Nusselt number.

Methodology

To perform this analysis, the Prandtl, Reynolds and Rayleigh numbers, as well as the total area of the cavity and the ratio between the total areas by the area of the fin, were kept constant.

For the computational development of this work, the ANSYS/Fluent® software was employed to solve the problem governor equations using the finite volume method, inherent to the software

Problem Description

The problem to be solved consists on analyzing the heat transfer in a cavity of square cross section with an elliptical fin inserted in the base of the section submitted to mixed convection. It was considered a two-dimensional domain, with the lateral surfaces and the base insulated, subjected to a velocity flow field that arises by the continuous movement of the upper plate on the cavity, besides the natural movement of the fluid caused by the differences in temperature in the flow thus characterizing the phenomenon of mixed convection.

A laminar, steady state and incompressible flow regime with the thermo-physical properties of the fluid and the flow constant throughout the domain was considered. Only the specific mass was not considered constant. In this case the Boussinesq approximation was applied. Figure 1 represents the domain of the problem to be studied together with the boundary conditions of the system.

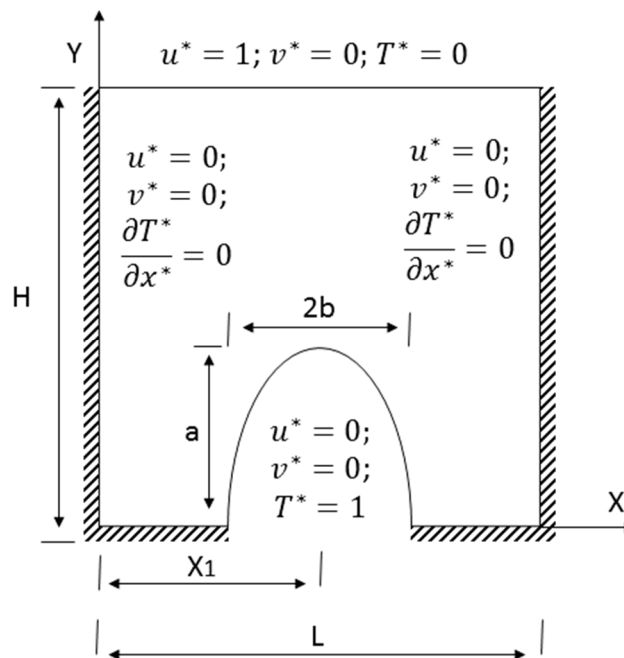


Figure 1. Representation of the computational domain and the boundary conditions of the problem.

As can be observed in the figure, the prescribed dimensionless temperature condition (Dirichlet boundary condition) was adopted for the upper plates and the fin, these being equal to $T^* = 0$ e $T^* = 1$ respectively. For the lateral surfaces, as well as the lower surface, they were considered as adiabatic surfaces (Neumann boundary condition), so that in this part of the domain we have $\partial T^*/\partial x^* = \partial T^*/\partial y^* = 0$. In addition, the non-slip and impermeability condition, $u^* = 0$ e $v^* = 0$, was adopted on all surfaces.

It was used the Constructal Law to determine the optimal geometry. Using this principle, we obtain the degrees of freedom of the problem, that is, the dimensions that vary according to predefined criteria. These predefined criteria were fixed as the total area of the cavity (A) and the fin area (A_f) and

these areas are calculated by Eq. (1) and Eq. (2). With the two areas it is possible to use a dimensionless relation given by Eq. (3) in order to facilitate the solution of the problem.

$$A = HL \quad (1)$$

$$A_f = \frac{\pi ab}{2} \quad (2)$$

$$\phi = \frac{A_f}{A} \quad (3)$$

From these relations of areas were also defined non-dimensional relationships for lengths and thus characterizing the entire domain. These dimensionless relations for the lengths are given by Eq. (4) to Eq. (7).

$$r = \frac{a}{b} \quad (4)$$

$$\tilde{a} = r\tilde{b} \quad (5)$$

$$\tilde{b} = \left(\frac{2\phi}{\pi r}\right)^{1/2} \quad (6)$$

$$\tilde{H}, \tilde{L} = \frac{\tilde{H}, \tilde{L}}{A^{1/2}} \quad (7)$$

Using the defined dimensionless lengths, the aspect ratio (r) was varied from 5 to 30 in order to find the best geometry for the problem. The values used are 5, 8, 12, 16, 20, 25 and 30. With the dimensions defined for the aspect ratio, the positioning of the fin on the axis (X_l) was varied. The positions adopted for X_l were from 0.1 to 0.9, in steps of 0.2.

In this way, it is possible to define the geometry since we have a fixed value for A and ϕ . Thus, it is possible to vary the shape of the fin in search of the optimal geometry by maximizing the average Nusselt number of the problem. These properties were used for the simulation of all geometries and positions along with the following fixed conditions: $H/L = 1$; $\phi = 0.05$; $Re_H = 10^2$; $Ra_H = 10^4$ and $Pr = 0.71$. The presented properties were taken from the database of the ANSYS/Fluent® software.

Mathematical and numerical formulation

The governing equations of the problem are the equations of continuity and momentum in the x and y directions, and also the energy equation (Schlichting and Gersten, 2000). These equations are represented respectively in Eq. (8) to Eq. (11) below:

$$\frac{\partial u}{\partial x} + \frac{\partial v}{\partial y} = 0 \quad (8)$$

$$u \frac{\partial u}{\partial x} + v \frac{\partial v}{\partial y} = -\frac{1}{\rho} \frac{\partial p}{\partial x} + \nu \left(\frac{\partial^2 u}{\partial x^2} + \frac{\partial^2 u}{\partial y^2} \right) \quad (9)$$

$$u \frac{\partial v}{\partial x} + v \frac{\partial v}{\partial y} = -\frac{1}{\rho} \frac{\partial p}{\partial y} + \nu \left(\frac{\partial^2 v}{\partial x^2} + \frac{\partial^2 v}{\partial y^2} \right) - g\beta(T - T_\infty) \quad (10)$$

$$u \frac{\partial T}{\partial x} + v \frac{\partial T}{\partial y} = \alpha \left(\frac{\partial^2 T}{\partial x^2} + \frac{\partial^2 T}{\partial y^2} \right) \quad (11)$$

where x and y represent the horizontal and vertical axis, respectively; u e v represent the velocities components horizontally and vertically, respectively; P represents the pressure; T is the temperature; T_∞ is the reference temperature, ρ represents the specific mass, α is the thermal diffusivity, ν is the kinematic viscosity; and β is the coefficient of thermal expansion.

By the same criterion for the characteristic lengths, we can still dimensionless the terms of temperature and speed in the axis. These dimensionless parameters can be found in Eq. (12) and Eq. (13):

$$\tilde{T} = \frac{T - T_{min}}{T_{max} - T_{min}} \quad (12)$$

$$(\tilde{u}, \tilde{v}) = \frac{(u, v)}{u_{max}} \quad (13)$$

Eq. (8) to Eq. (11) are solved numerically by the commercial software ANSYS/Fluent®. The software solves these equations using the Finite Volume Method. This discretization method is based on dividing the total volume into smaller control volumes such that each control volume has a point in the mesh, so the differential equation is integrated into each volume thus representing variations in the amount of movement, energy and balance of mass at each point (Patankar, 1980). In the software it was also possible to apply the SIMPLE method in order to solve the pressure-velocity couplings of the equations. The spatial discretization used for momentum and energy was the power law, and for pressure,

the body force weighted method. As convergence criteria, values of 10^{-6} were used for mass and momentum conservation and 10^{-8} for energy conservation.

Bejan (2004) defines convective heat flow per unit area as the product of the heat transfer coefficient by the temperature difference, as shown in Eq. (14):

$$q'' = h(T - T_{\infty}) \quad (14)$$

where q'' is the heat flux (W/m^2); h the heat transfer coefficient ($\text{W}/\text{m}^2 \cdot \text{K}$); and $(T - T_{\infty})$ is the temperature difference between the fluid and the fin (K).

Some relationship is also necessary in order to relate the boundary layer. For the boundary layer, the dimensionless Reynolds number was adopted based on the height of the cavity. The Reynolds number describes the type of flow, laminar or turbulent and is defined as:

$$Re_H = \frac{\rho u_{max} H}{\mu} \quad (15)$$

where u_{max} is the velocity of the upper movable plate (m/s); and μ is the dynamic viscosity of the fluid (m^2/s) (Schlichting and Gersten, 2000). The Reynolds number was kept fixed in all performed simulations.

It is still necessary to characterize the natural convection in the heat transfer from the fluid. Thus, the Rayleigh number was used to define this aspect. When the Rayleigh number value is less than the critical value of the flow, this indicates that the heat transfer occurs mainly by diffusion. Values above this critical value indicate that heat transfer occurs by convection (BEJAN, 2004). The Rayleigh number was kept constant during all simulations, being defined by:

$$Ra_H = \frac{g\beta(T - T_{\infty})H^3}{\nu\alpha} \quad (16)$$

where g corresponds to gravity acceleration; and β is the thermal expansion coefficient.

Results and Discussion

Grid Independence Analysis

In the mesh independence analysis, it is established the grid in which the refinement does not significantly interfere on the results numerically obtained. To evaluate the mesh independence, it was made five different meshes with different discretizations. The average Nusselt number was calculated for each discretization level and the normalized deviation between each result was obtained. From these values, one obtains the grid elements dimension that will be use in all simulations.

Table 1 shows the results for the average Nusselt number in function of mesh elements and the size of the element face, together with the difference in relation to the result obtained when using the dimension of the element immediately inferior. The chosen data to this study was $X_l = 0.5$ and $r = a/b = 1$.

From Tab. 1 it can be seen that the difference of determined values for average Nusselt number decreases to successive larger discretization, except for the last value. As shown in Tab. 1 one mesh with size of face of element of 0.01 entails the difference of 0.015% between the results. For more refined mesh the computational time is greater, as well as the difference between the results. In this way, the discretization with 0.01 of element size was maintained because the obtained results are good enough and the computational time is reasonable.

Table 1. Grid independence in relation to average Nusselt number.

Size of face (mm)	Elements	\overline{Nu}	$\left \frac{\overline{Nu}^i - \overline{Nu}^{i+1}}{\overline{Nu}^i} \right $
0.02	2779	3.3644	0.00095
0.01	9780	3.3676	0.00015
0.009	11958	3.3671	0.00030
0.008	15026	3.3670	-

Computational model validation

After determining the discretization of the domain that will be used, the simulation was performed with the different parameters that influence the average Nusselt number. However, it was necessary to validate the results before the simulations. To validate the numerical code, it was used the results of previous studies. To do so, the results obtained in this work were compared with the results obtained by Calderaro (2015) and Machado (2014).

The variables used in this validation was $X_l = 0.5$ and $r = 1$. The remaining properties were maintained the same as the properties found in the work of Calderaro (2015).

In the work of Calderaro (2015) the superior wall of the domain is not mobile. Changing this boundary condition and using the same conditions of the validation problem on the present code, the obtained results are in good agreement with those presented in Calderaro (2015). In the work of Machado (2014), the fin is a rectangle. The properties used are: $\phi = 0.05$, $Re_H = 1000$, $Ra_H = 10^6$, $Pr = 0.71$, $H_1/L_1 = 0.5$. The differences between the code used in this work, and that used by Calderaro (2015). and Machado (2014), can be seen in Tab. 2.

Table 2. Computational model validation.

	\overline{Nu}	Percentage Difference
Present Work	12.80	1.56%
Calderaro (2015)	12.60	
Present Work	14.22	0.91%
Machado (2014)	14.35	

Average Nusselt number variation

In this section, the main results will be show. At first, the variance of the average Nusselt number is shown according with the fin position inside of the cavity (X_f) and with the eccentricity relation of the fin, defined by $r = a/b$.

In Figure 2 is presented the variation of the average Nusselt number in function of the fin eccentricity (r).

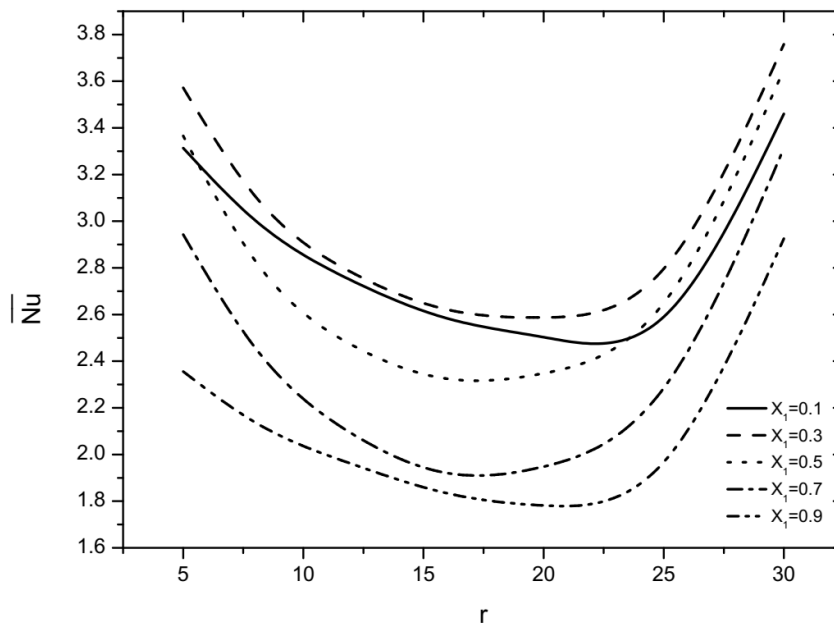


Figure 2. Average Nusselt number in function of fin eccentricity.

Analyzing Fig. 2, it is possible to note that the average Nusselt number tends to be minimized to r values between 15 and 20, for the values of eccentricity of 0.3, 0.5 and 0.7, and to r values between 20 and 25, for the values of eccentricity of 0.1 and 0.9. The values of the average Nusselt number tends to be maximized to values of r close to 30. As the Nusselt number provides the relationship between convection heat transfer and conduction heat transfer, it has been shown that one way to increase the convection heat transfer is to increase the eccentricity of the fin to values close to 30 or lower than 10 in the most of the cases. Intermediate values generally decrease the convection heat transfer.

The maximum values of the average Nusselt number are obtained in the position between $X_I = 0.3$ and 0.5 , for the most of the cases. This fact is shown on the Fig. 3, then to maximize the average Nusselt number, and consequently the heat transfer by convection, the fin should be positioned near the position where $X_I = 0.3$.

That is, to maximize the average Nusselt number, and consequently the convection heat transfer, must be chosen fins with eccentricities close to 5 or 30, and position them near to $X_I = 0.3$. Thus, and from the analysis of the graphs, we note that the case that maximizes the average Nusselt number is the case where $r = 30$ and $X_I = 0.3$. This case can be seen in Fig. 7.

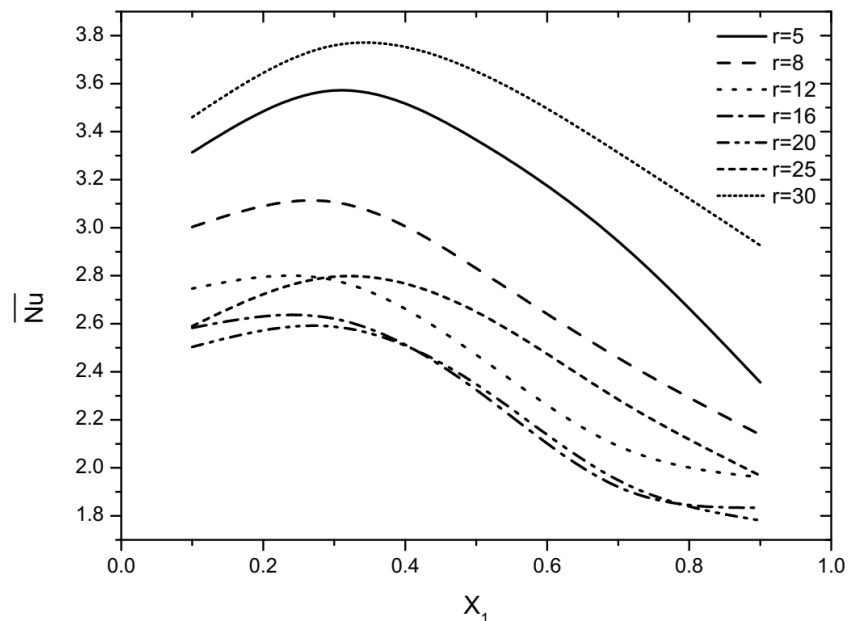


Figure 3. Average Nusselt number in function of fin position in the domain.

The values obtained to average Nusselt number in symmetric positions in relation of the domain center are not equal, for example, to the position $X_I = 0.1$, with $r = 5$, the value was $\overline{Nu} = 3.3135$, while to the position $X_I = 0.9$, the value was $\overline{Nu} = 2.3560$.

The fact that can explain these differences is the movable wall on the top of the domain. This wall can move in the domain direction that goes from zero to one on the x direction, which is coincident to the X_I direction. Due to this fact, fluid in an inferior temperature than the fin is moved inside the domain, in direction of higher values of X_I thus decreasing the temperature difference that exist between the fin and the fluid, reducing the Nusselt number. This behavior is illustrated in Fig. 4.

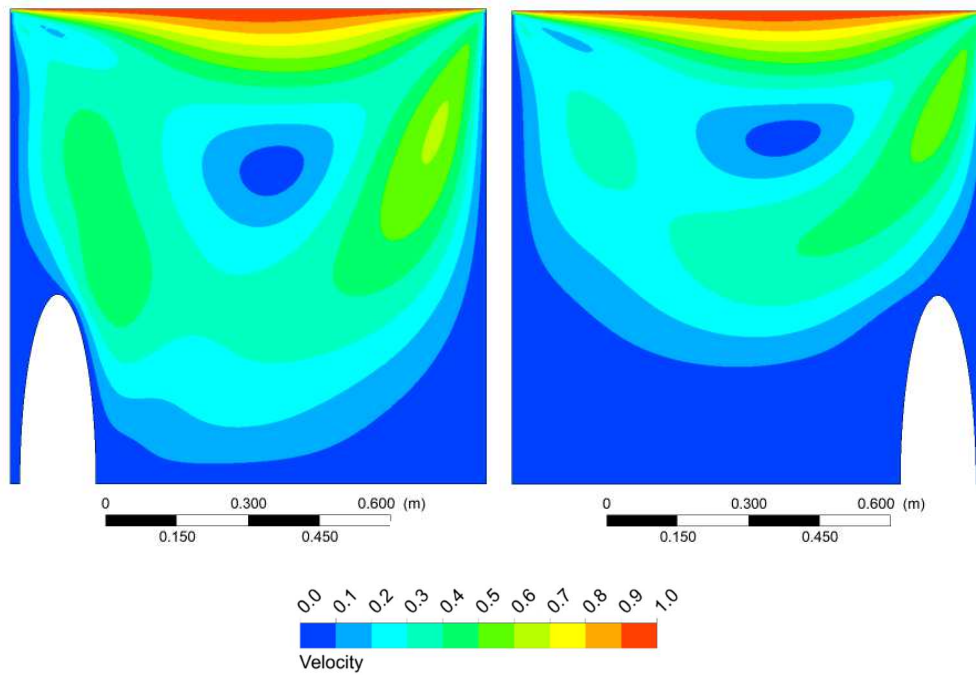


Figure 4. Velocity contours to $X_1 = 0.1$ (left) and $X_1 = 0.9$ (right), with $r = 5$.

From the above mentioned fact and the analysis of Fig. 4 it is possible a better understanding of the temperature distribution that is shown in Fig. 5. This analysis corroborates the results to the average Nusselt number variation according with fin location inside the domain.

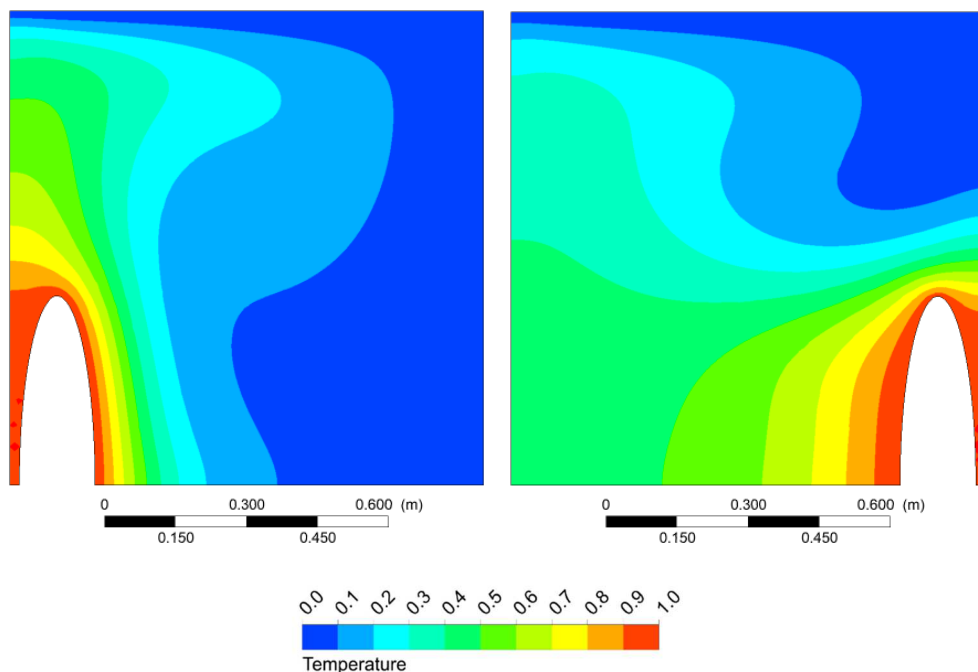


Figure 5. Temperature contours for $X_1 = 0.1$ (left) and $X_1 = 0.9$ (right), with $r = 5$.

Analyzing Fig. 6, the velocity contours (above) and the temperature (below) can be observed for the fin at $X_1 = 0.5$ position with eccentricity equal to 5 and 25, respectively. From the velocity distribution it can be noted that the fin with larger eccentricity have a larger fluid circulation near the top extremity.

In the fin with smaller eccentricity, this phenomenon is smaller too. This fact explains the increase of the average Nusselt number for the higher eccentricity of the fin.

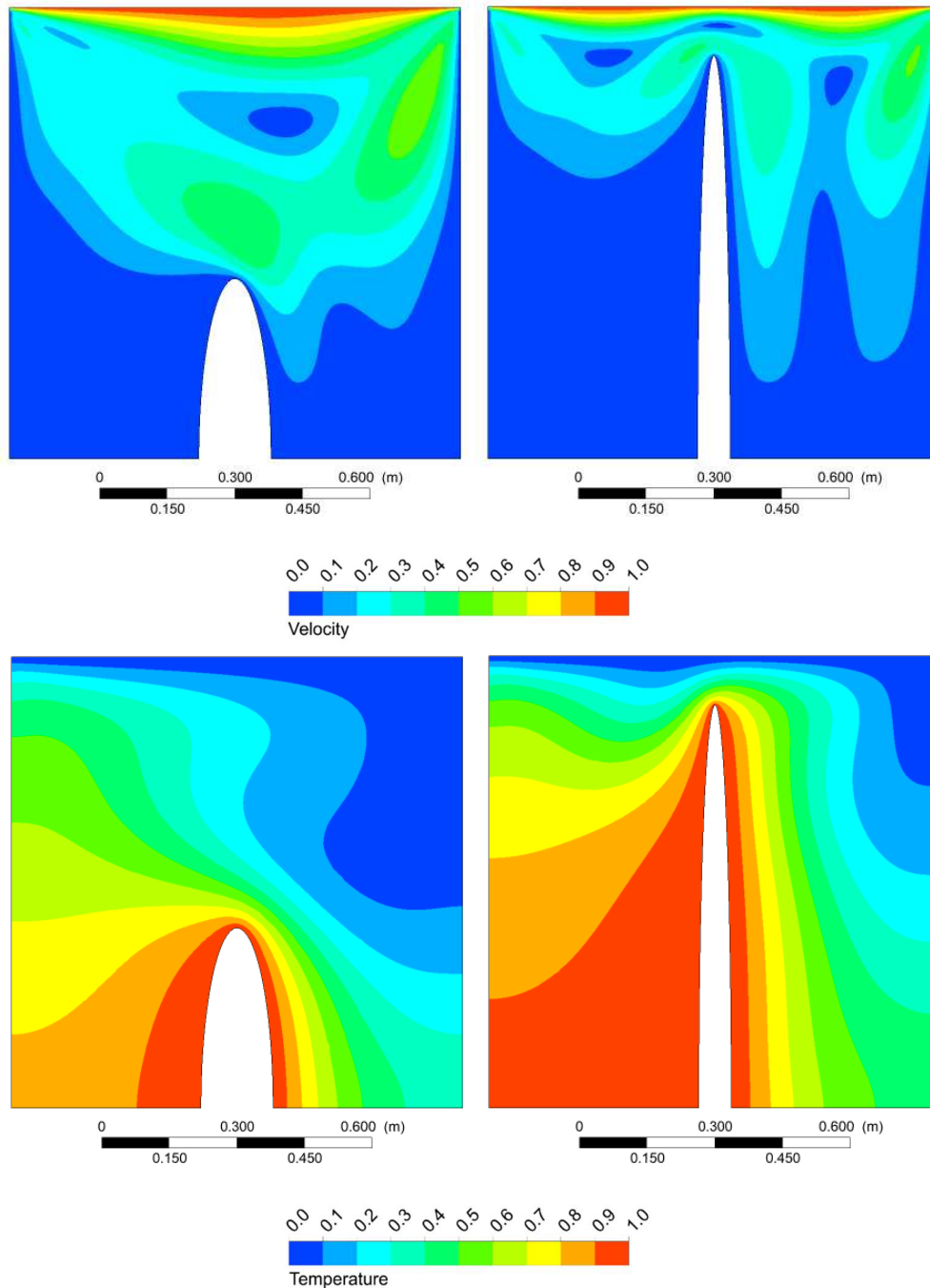


Figure 6. Velocity contour (above) and temperature contour (below) for eccentricity of 5 (left) and 25 (right), with $X_1 = 0.5$.

The cases where the highest and lowest Nusselt number were obtained, respectively, were those with $r = 30$ and $X_1 = 0.3$ with $\overline{Nu} = 3.7592$ and $r = 20$ and $X_1 = 0.9$ with $\overline{Nu} = 1.7812$.

Therefore, comparing the geometries with the higher and smaller average Nusselt number, we can see a difference around 50%. Figure 7 presents the distribution of temperature and velocity for these two cases.

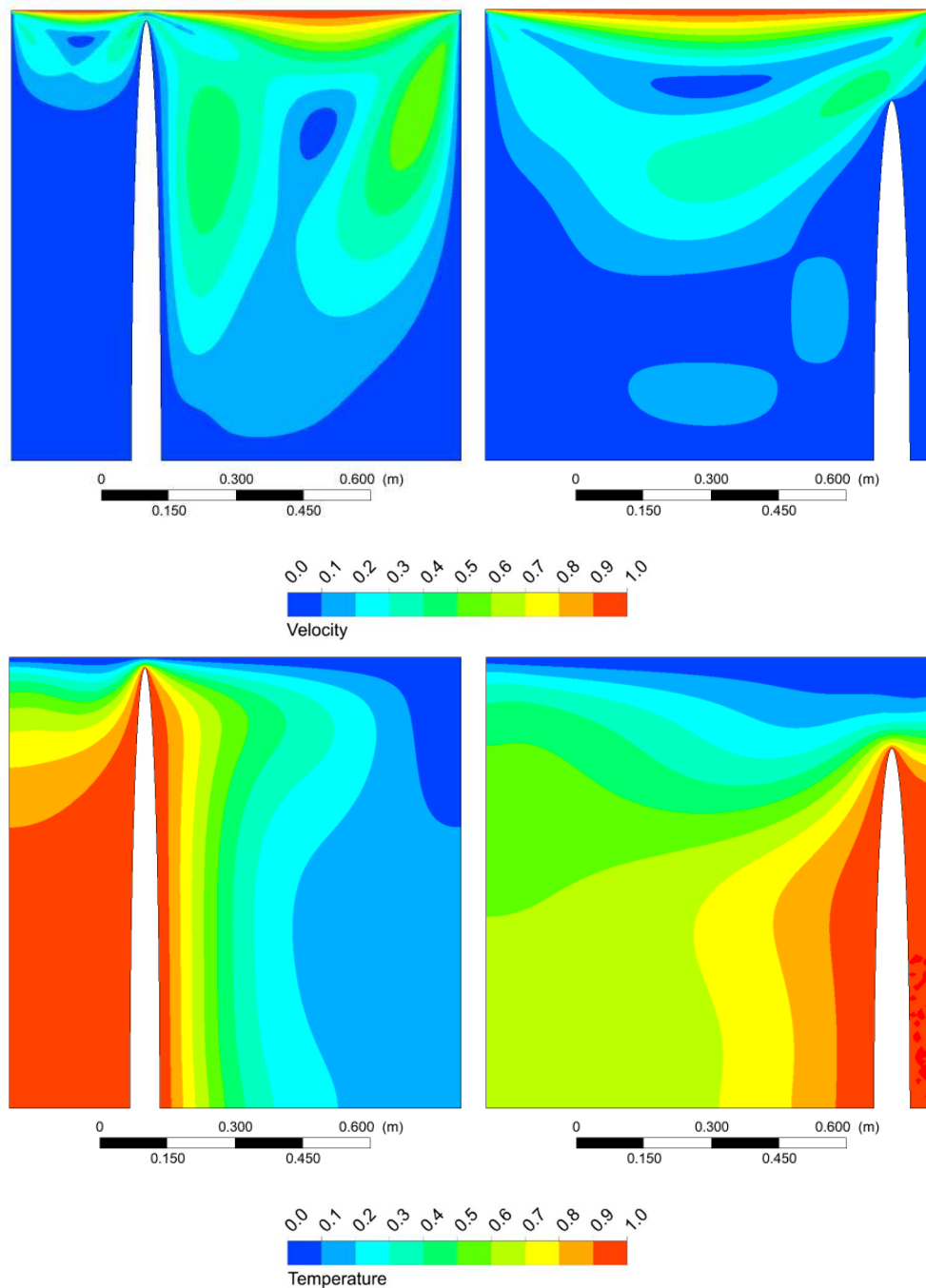


Figure 7. Cases where the highest Nusselt number (left) and the lowest Nusselt number (right) were found. Left ($r = 30$ and $X_1 = 0.3$ with $\overline{Nu} = 3.7592$). Right ($r = 20$ and $X_1 = 0.9$, with $\overline{Nu} = 1.7812$).

The case with the lower average Nusselt number ($r = 20$ and $X_1 = 0.9$), can be explained through figure 7. As the fin lies at the end of the domain, there is only relevant fluid circulation on one side of the geometry, which ultimately decreases the convection heat transfer.

Conclusion

In this work, a mixed convection in an elliptical fin was studied. The A and B axis have a variable dimension, however the relation of the domain areas of the fin was maintained constant. The problem

conditions are a bottom surface with higher temperature and a top surface with lower temperature. The top surface moves with a certain velocity in the positive direction of the x-axis. All the others surfaces are isolated.

The software ANSYS/Fluent® was used to solve this engineering problem. A mesh independency study was performed. This study was made to define the ideal relation between mesh and necessary computational time to solve the problem. The results were validated based in past studies. (Calderaro, 2015; Machado, 2014).

The obtained results showed that the average Nusselt number has a relation with fin position inside the domain. The results also shown the same dependence for the fin eccentricity. It was observed that the fin position around $X_f = 0.3$ presented the higher values for the average Nusselt number, as well as the eccentricities close to 5 and 30. Due to the movement of the top surface, which moves fluid at a lower temperature around the domain, the average Nusselt number distribution is not symmetric.

For the same fin position inside the domain it was noticed that the average Nusselt number varies according to the fin eccentricity, presenting a minimum point for eccentricity values around 15, for the fin positions of 3, 5 and 7, and around 20 for the fin positions of 1 and 9, being maximum for values close to 30, for all the cases.

The numerical method was of fundamental importance to accomplish this study, considering its potential repeatability and good correlation of results with physical aspects. Results obtained are of great value for future studies with different boundary conditions and different parameters to be evaluated. Once again, the study ends up corroborating the results expected from the study of the Constructal Law, since the studied parameters have optimal points for certain conditions.

Acknowledgements

We would like to thank CAPES, CNPq and Federal University of Rio Grande do Sul for their resources.

References

- BEJAN, A.; LORENTE, S. 2004. The constructal law and the thermodynamics of flow systems with configuration. *International journal of heat and mass transfer*, **47**(14-16):3203–3214. <https://doi.org/10.1016/j.ijheatmasstransfer.2004.02.007>
- BEJAN, A. 2004. *Shape and Structure, from Engineering to Nature*. Cambridge, Cambridge University Press, 325 p.
- BEJAN, A. 2004. *Convection Heat Transfer*. Hoboken, NJ, Wiley, 696 p.

- BEJAN, A.; KRAUS, A.D. 2003. *Heat Transfer Handbook*. Hoboken, NJ, John Wiley & Sons, 1479 p.
- BEJAN, A.; LORENTE, S. 2006. Constructal theory of generation of configuration in nature and engineering. *Journal of Applied Physics*, **100**(4):041301. <https://doi.org/10.1063/1.2221896>
- BEJAN, A.; LORENTE, S. 2008. *Design with constructal theory* Hoboken, Hoboken, NJ, John Wiley & Sons, 744 p.
- BEJAN, A.; ZANE, J. P. 2013 *Design in Nature: How the Constructal Law Governs Evolution in Biology, Physics, Technology, and Social Organizations*. Reprint ed., Nova York, NY, Anchor Books, 1071 p.
- CALDERARO, J.C. *Estudo numérico da convecção natural sobre uma aleta elíptica aquecida no interior de uma cavidade*. 2015. Porto Alegre, RS. Trabalho de Conclusão de Graduação. Universidade Federal do Rio Grande do Sul (UFRGS), 17 P. <http://hdl.handle.net/10183/132682>
- ÇENGEL, Y. A.; GHAJAR, A. J. 2011. *Heat and Mass Transfer Fundamentals and Applications*. New York, NY, McGraw Hill, 957 p.
- LORENZINI, G. et al. 2016. Constructal design of rectangular fin intruded into mixed convective lid-driven cavity flows. *Journal of Heat Transfer*, **138**(10):102-501. <https://doi.org/10.1115/1.4033378>
- LORENZINI, G. et al. 2012. Constructal design applied to the optimization of complex geometries: T-Y-shaped cavities with two additional lateral intrusions cooled by convection. *International Journal of Heat and Mass Transfer*, **55**(5):1505–1512. <https://doi.org/10.1016/j.ijheatmasstransfer.2011.10.057>
- LORENZINI, G.; ROCHA, L.A.O. 2009. Geometric optimization of T-Y-shaped cavity according to Constructal design. *International Journal of Heat and Mass Transfer*, **52**(21-22):4683–4688. <https://doi.org/10.1016/j.ijheatmasstransfer.2009.06.020>
- MACHADO, B. de S. 2014. *Constructal design de aleta retangular inserida em cavidade com superfície superior deslizante sob efeito de convecção mista*. Porto Alegre, RS. Dissertação de Mestrado. Universidade Federal do Rio Grande do Sul (Ufrgs), 82 p. <http://hdl.handle.net/10183/108489>
- NETO, D.C. et al. 2010. Numerical analysis of buoyancy in mixed convection heat transfer in lid-driven cavity flows. In: Proceedings of 13th Brazilian Congress of Thermal Sciences and Engineering, 13, Uberlândia, 2010.
- PATANKAR, S. 1980. *Numerical heat transfer and fluid flow*. USA, CRC press, 214 p.
- SCHLICHTING, H.; GERSTEN, K. 2000. *Boundary-Layer Theory*. Springer, Berlin, 805 p.

Submetido: 09/06/2017

Aceito: 03/01/2018